

## GRB 010921: Discovery of the First HETE Afterglow

P. A. Price<sup>1,2</sup>, S. R. Kulkarni<sup>1</sup>, E. Berger<sup>1</sup>, S. G. Djorgovski<sup>1</sup>, D. A. Frail<sup>1,3</sup>, A. Mahabal<sup>1</sup>, D. W. Fox<sup>1</sup>, F. A. Harrison<sup>1</sup>, J. S. Bloom<sup>1</sup>, S. A. Yost<sup>1</sup>, D. E. Reichart<sup>1</sup>, A. A. Henden<sup>4</sup>, G. R. Ricker<sup>5</sup>, R. van der Spek<sup>5</sup>, K. Hurley<sup>6</sup>, J.-L. Atteia<sup>7</sup>, N. Kawai<sup>8,9</sup>, E. Fenimore<sup>10</sup> & C. Graziani<sup>11</sup>.

### ABSTRACT

We report the discovery of the optical and radio afterglow of GRB 010921, the first gamma-ray burst afterglow to be found from a localization by the High Energy Transient Explorer (HETE) satellite. We present optical spectroscopy of the host galaxy which we find to be a dusty and apparently normal star-forming galaxy at  $z = 0.451$ . The unusually steep optical spectral slope of the afterglow can be explained by heavy extinction,  $A_V > 0.5$  mag, along the line of sight to the GRB. Dust with similar  $A_V$  for the host galaxy as a whole appears to be required by the measurement of a Balmer decrement in the spectrum of the host galaxy. Thanks to the low redshift, continued observations of the afterglow will enable the strongest constraints, to date, on the existence of a possible underlying supernova.

---

<sup>1</sup>Palomar Observatory, 105-24, California Institute of Technology, Pasadena, CA, 91125.

<sup>2</sup>Research School of Astronomy & Astrophysics, Mount Stromlo Observatory, via Cotter Road, Weston, ACT, 2611, Australia.

<sup>3</sup>National Radio Astronomy Observatory, P.O. Box O, Socorro, NM, 87801.

<sup>4</sup>Universities Space Research Association / US Naval Observatory, Flagstaff Station, P.O. Box 1149, Flagstaff, AZ, 86002-1149

<sup>5</sup>Center for Space Research, Massachusetts Institute of Technology, Cambridge, MA, 02139-4307

<sup>6</sup>University of California Space Sciences Laboratory, Berkeley, CA, 94720.

<sup>7</sup>Centre d'Etude Spatiale des Rayonnements, CNRS/UPS, B.P. 4346, 31028 Toulouse Cedex 4, France.

<sup>8</sup>Department of Physics, Faculty of Science, Tokyo Institute of Technology, 2-12-1 Ookayama, Meguroku, Tokyo 152-8551, Japan.

<sup>9</sup>RIKEN (The Institute of Physical and Chemical Research), 2-1 Hirosawa, Wako, Saitama 351-0198, Japan.

<sup>10</sup>MS D436, Los Alamos National Laboratory, Los Alamos, NM 87545.

<sup>11</sup>Department of Astronomy and Astrophysics, University of Chicago, 5640 South Ellis Avenue, Chicago, IL 60637.

*Subject headings:* gamma rays: bursts

## 1. Introduction

The High Energy Transient Explorer (HETE-2) was successfully launched and deployed on 2000 October 9 (Ricker et al. 2000). As the first satellite entirely dedicated to the detection and study of gamma-ray bursts (GRBs), HETE’s primary mission is the localization of GRBs through their prompt emission and the rapid relaying of the coordinates to ground-based observers. Here, we present the discovery of the afterglow of GRB 010921 (Ricker et al. 2001b), the first afterglow to be identified through localization by HETE-2.

## 2. Discovery of an Optical and Radio Transient

GRB 010921 triggered the FREGATE instrument on board HETE-2 on 2001 September 21.21934 UT as HETE trigger number 1761 (Ricker et al. 2001a). The GRB was detected by only one of HETE’s two Wide-field X-ray Monitors, and so localization was only possible in a single dimension. Fortunately, the Interplanetary Network was able to provide complementary localization and the resultant 310-square-arcmin error box was speedily reported to the community via the GRB Coordinate Network (GCN) Circulars (Hurley et al. 2001). We observed this error box with the Large Format Camera (LFC) on the Hale 200-inch telescope at Palomar Observatory, commencing 22 hours after the GRB, in the Sloan Digital Sky Survey (SDSS; York et al. 2000)  $r'$  filter. Despite the 26-arcmin field-of-view (FOV) of the LFC, three pointings were required to cover the entire error box.

A quick comparison of the images with the Digital Palomar Observatory Sky Survey (Djorgovski et al. 1999; also in prep.) failed to identify an afterglow candidate within the large error box (Fox et al. 2001). Hoping to identify the afterglow by its variability (i.e., decay), we re-observed the error box with LFC five days later.

Reduction of data from LFC is complicated by the instrument’s large FOV which leads to substantial optical distortions in the focal plane, some of which can be removed in software, but this does not correct for the inevitable coma at the edges of the field. Furthermore, this problem is made worse by our choice of on-chip binning (which however reduced the file size of the images). We used the MSCRED package in the Image Reduction and Analysis Facility (IRAF)<sup>12</sup> to bias-subtract, flat-field and combine the individual images.

---

<sup>12</sup>IRAF is distributed by the National Optical Astronomy Observatories.

Comparison of the first- and second-epoch images was done through PSF-matched image subtraction (Alard 2000). Subtraction of images was rendered difficult due to the binning of pixels. Nonetheless, we identified source A ( $\alpha_{2000} = 22^{\text{h}}55^{\text{m}}59^{\text{s}}90$ ,  $\delta_{2000} = +40^{\circ}55'52''9$ ) and source B ( $\alpha_{2000} = 22^{\text{h}}56^{\text{m}}15^{\text{s}}09$ ,  $\delta_{2000} = +41^{\circ}04'48''1$ ), both of which were within the error box and were clearly variable. These positions are derived relative to USNO-A2.0 and are uncertain by approximately 0.6 arcsec.

In order to further investigate these two sources, we re-observed the field on 2001 October 12th and 17th, 21 and 26 days after the GRB respectively. Photometry from these epochs revealed that source B had increased in brightness, while source A had faded further and appeared to be settling to a constant flux level; see Figures 1 and 2. Source B, which is faintly visible at the plate limit of the second Digitised Sky Survey<sup>13</sup>, is likely a variable star or some other object unrelated to the GRB, while the light curve of source A bears a similarity to the afterglows of other GRBs which are observed to undergo a power-law decay followed by leveling off at the flux level of the host galaxy.

Optical photometry was performed relative to stars in the field calibrated through observations of numerous Landolt standards observed at the USNO Flagstaff Station 1.0-meter telescope on 2001 September 22. We estimate that these calibrations have a zero-point error of less than 0.03 mag. Reference star magnitudes in the SDSS photometric system were derived through application of the transformations of Fukugita et al. (1996). The resulting photometry of source A can be found in Table 1.

A program of observations at the Very Large Array (VLA)<sup>14</sup> were begun commencing on 2001 October 17; see Table 2. All radio observations were obtained in the standard continuum mode with  $2 \times 50$  MHz contiguous bands. We observed the extra-galactic source J2255+420 for phase calibration, and 3C48 (J0137+331) and 3C286 (J1331+305) for flux calibration. All data were reduced using the Astronomical Image Processing System (AIPS).

Coincident with source A, we identified a radio source at  $\alpha_{2000} = 22^{\text{h}}55^{\text{m}}59^{\text{s}}931 \pm 0.018$  and  $\delta_{2000} = +40^{\circ}55'52''23 \pm 0.20$  and with a spectral slope of  $\beta = 0.35 \pm 0.19$  (where  $f_{\nu} \propto \nu^{\beta}$ ) between 4.86 and 22.5 GHz. This value of  $\beta$  is consistent with that expected from the synchrotron emission of an afterglow ( $\beta = 1/3$ ; Sari, Piran & Narayan 1998), but does not exclude the possibility that the source is a low-luminosity AGN. Further observations indicate variability in the source (Table 2), which may be interpreted as due to interstellar

---

<sup>13</sup>The Digitized Sky Surveys were produced at the Space Telescope Science Institute under U.S. Government grant NAG W-2166.

<sup>14</sup>The National Radio Astronomy Observatory (NRAO) is a facility of the National Science Foundation operated under cooperative agreement by Associated Universities, Inc. NRAO operates the VLA.

scintillation, a phenomenon commonly seen in radio afterglows (Frail et al. 1997).

### 3. The Afterglow

As noted above, the optical light curve, a decline followed by leveling off, the variable radio emission and the flat radio spectrum, support the identification of source A as the afterglow of GRB 010921. However, the data are sparse and the possibility remains that source A could be an AGN since AGNs also possess power-law spectra and can be strongly variable. However, in section 4 we note that the optical spectrum of the host does not show any evidence for a central engine. Furthermore, by comparing Palomar LFC images taken on 2001 September 22 (dominated by the optical transient) with those taken on 2001 October 17 (dominated by the galaxy), we find that the transient is offset from the light centroid of the host galaxy by  $0.351 \pm 0.049$  arcsec, or  $2.18 \pm 0.30$  kpc at the distance of the galaxy (see §4). Such angular and physical offsets with respect to their host galaxy are typical of GRBs (Bloom, Kulkarni & Djorgovski 2002). Thus from the totality of the radio and optical data we concluded that source A is not an AGN but rather the afterglow of GRB 010921 and announced it as such (Price et al. 2001b).

After accounting for Galactic extinction towards this direction ( $E_{(B-V)} = 0.148$ ; Schlegel, Finkbeiner & Davis 1998) we fit the optical photometric measurements to a power-law (afterglow) model,  $F_\nu \propto t^\alpha \nu^\beta$ . We obtain marginally-acceptable fits ( $\chi^2/\text{DOF} = 14.5/10$ ), with  $\alpha = -1.59 \pm 0.18$  and  $\beta = -2.22 \pm 0.23$ . Park et al. (2002) report similar decay values based on observations carried out with a number of telescopes.

The temporal decay slope is consistent with those seen in previous optical afterglows, but the spectral slope is quite steep, suggestive of extinction in the source frame. Adopting standard afterglow theory (Sari, Piran & Narayan 1998), we can deduce the intrinsic spectral slope from the temporal data. However, this inference depends on the details of the afterglow model (ambient gas, homogeneous versus inhomogeneous; the electron distribution power law index,  $p$ ; the shape of the explosion, spherical versus collimated outflow). The extinction along the line-of-sight to the GRB, parametrized by  $A_V$  in the rest frame of the source, can then be obtained from the deviation of the observed broad-band spectrum from that expected from the afterglow model.

The actual value of the derived  $A_V$  is somewhat dependent on the choice of both the extinction curve (Milky Way, LMC or SMC), and the afterglow model (collimated or isotropic ejecta; cooling break, redward or blueward of the optical band over the course of the observations) but, as can be seen from Table 4 it is clear that  $A_V$  is in excess of 0.5 mag. The

best fit model has a spherical outflow with the cooling frequency below the optical band by day 1 and an LMC-like extinction curve ( $\chi^2/\text{DOF} = 15.5/11$ ).

#### 4. The Host Galaxy

Using the Double Spectrograph (Oke & Gunn 1982) at the Cassegrain focus of the Hale 200-inch telescope we obtained a spectrum of the host galaxy (Figure 3). We used a 1-arcsec wide long-slit, at a position angle  $132^\circ$ , close to the parallactic angle, and a  $158 \text{ lines mm}^{-1}$  grating, giving an effective instrumental resolution  $\text{FWHM} \approx 12 \text{ \AA}$ , and an approximate wavelength coverage  $5,000\text{--}10,000 \text{ \AA}$  on the red side. We obtained 2 exposures of 1800-s each, with a small dither along the slit. Exposures of arc lamps were obtained for calibrations and small wavelength shifts due to the instrument flexure were removed by fitting the wavelengths of night sky lines. The net resulting wavelength scatter is  $\sim 0.4 \text{ \AA}$ . Flux calibration was made through observations of the spectrophotometric standard BD+17°4708 from Oke & Gunn (1983).

Several emission lines are detected (see Table 3), corresponding to  $[\text{O II}]\lambda 3727$ ,  $\text{H}\beta$ ,  $[\text{O III}]\lambda\lambda 4959, 5007$  and  $\text{H}\alpha$ , at a mean redshift of  $z = 0.4509 \pm 0.0004$ . We note that the widths of the lines, ranging from  $10 \text{ \AA}$  to  $13 \text{ \AA}$ , are consistent with the instrumental resolution and thus there is no reason to invoke an AGN component to this host galaxy. Furthermore, the line flux ratios  $F_{5007}/F_{4861}$  and  $F_{3727}/F_{5007}$  place the host galaxy squarely in the range corresponding to normal HII galaxies on the identification plot of Baldwin, Phillips & Terlevich (1981).

In estimating the properties of the host galaxy, we adopt a standard flat cosmology with  $H_0 = 65 \text{ km s}^{-1} \text{ Mpc}^{-1}$ ,  $\Omega_M = 0.3$  and  $\Omega_\Lambda = 0.7$ . From the observed Balmer decrement and an LMC extinction curve, we calculate an optical depth at  $\text{H}\beta$  due to dust of 1.51 (assuming an intrinsic  $\text{H}\alpha$  to  $\text{H}\beta$  flux ratio of 2.87; Mathis 1983); note, we have not accounted for Balmer absorption lines in the host galaxy. The corresponding  $A_V$  which applies to the galaxy as a whole is 1.3 mag. This value of  $A_V$  is comparable to the extinction along the line-of-sight to the GRB afterglow and thus most likely the extinction observed in the afterglow is due to interstellar (as opposed to circumburst) dust.

There are two other GRB host galaxies for which Balmer line fluxes have been published, the hosts of GRBs 980703 (Djorgovski et al. 1998) and 990712 (Vreeswijk et al. 2001), for which we calculate optical depths at  $\text{H}\beta$  of approximately 0.1 and 2.41, respectively, using the above method. We note that the Balmer decrement observed for the host of GRB 010921 falls squarely within the range observed for these other two GRB hosts.

We now infer the metallicity (oxygen abundance) using the empirical relation between oxygen abundance and  $\log R_{23} \equiv \log ([OII] + [OIII])/H\beta$  (Kobulnicky, Kennicutt & Pizagno 1999). We find  $\log R_{23} = 1.05 \pm 0.18$  which is close to the knee of this relation and thus yields an unambiguous measure of the oxygen abundance,  $12 + \log (O/H)$  of  $8.35 \pm 0.25$ . The rest-frame equivalent width of the [O II] line,  $34.5 \pm 3.5 \text{ \AA}$ , is typical for field galaxies (Hogg et al. 1998), which have equivalent widths spanning  $0 - 50 \text{ \AA}$ . Furthermore, using the [O II] and  $H\alpha$  line fluxes and the empirical star-formation rate (SFR) estimators of Kennicutt (1998) we derive extinction-corrected SFR of  $8 M_{\odot} \text{ yr}^{-1}$  and  $6 M_{\odot} \text{ yr}^{-1}$  respectively. All in all, we conclude that GRB 010921 occurred in a normal, star-forming galaxy with an oxygen abundance approximately one-quarter solar.

We also observed the host galaxy with the Near InfraRed Camera (NIRC; Matthews & Soifer 1994) on the Keck I telescope on 2001 November 1 UT in the  $JHK_s$  bands under photometric conditions. The individual frames were flat-fielded and then sky-subtracted and combined using the DIMSUM package in IRAF (Eisenhardt et al. 1999). Flux calibration was performed through observation of Persson et al. (1998) standards SJ9126 and SJ9134. We estimate that the calibration is accurate to within 0.05 mag. The resulting magnitudes of the host galaxy, measured within a 1.5-arcsec aperture, are also displayed in table 1. From the flat spectrum in the NIR, we estimate that the stellar population of the host is less than 1 Gyr in age.

From the FREGATE 8–400 keV fluence of  $1.5 \times 10^{-5} \text{ erg/cm}^2$  (Ricker et al. 2001b), we derive the isotropic-equivalent prompt energy release (without any k correction) of  $9.0 \times 10^{51} \text{ erg}$ . However, it is now generally appreciated that GRBs are beamed or collimated (Frail et al. 2001) and thus the isotropic-equivalent value is an upper limit. Unfortunately, the paucity of the afterglow data do not place significant constraint on the opening angle of the explosion (see Table 4).

## 5. Conclusion

Here we report the first afterglow resulting from an HETE localization of a GRB. The afterglow in itself is similar to afterglows studied to date. However, the GRB occurred in a low-redshift,  $z = 0.451$ , dusty star-forming galaxy. Such low redshift GRBs are valuable for two reasons. First and foremost, such low-redshift events offer the best opportunity to study the explosion physics including the opportunity to constrain the presence of (or detect) any underlying supernova. Second, the low redshift allowed us to determine the metallicity of the host galaxy with relative ease.

It is perhaps significant to note that the afterglow was discovered through the use of image differencing. We suggest that the use of this technique may be a more robust method of identifying GRB afterglows than the traditional manual comparison with sky survey images, since it enables the detection of an afterglow superimposed on a bright host galaxy. This is particularly important for low redshift GRBs. We wonder whether the traditional approach — looking for an isolated transient — could be the cause of failure to identify optical afterglows in some GRBs.

We thank Martha Haynes for the generous donation of her Hale 200-inch time without which the discovery of this afterglow would not have been possible. We thank Rick Burrus for his help with 200-inch observations. PAP gratefully acknowledges an Alex Rodgers Travelling Scholarship. DAF thanks Caltech for the hospitality shown by Caltech during his sabbatical leave. SRK and SGD thank NSF for support of our ground-based GRB observing program. JSB acknowledges support from the Hertz Foundation in the form of a fellowship. KH is grateful for *Ulysses* support under Contract JPL 958059, and for HETE support under Contract MIT-SC-R-293291.

## REFERENCES

- Alard, C. 2000, A&AS, 144, 363.
- Baldwin, J.A., Phillips, M.M. & Terlevich, R. 1981, PASP, 93, 5.
- Berger, E. et al. 2001, ApJ, 556, 556.
- Bloom, J. S., Djorgovski, S. G. & Kulkarni, S. R. 2002, ApJ, 554, 678.
- Bloom, J. S., Kulkarni, S. R. & Djorgovski, S. G. 2002, AJ (in press).
- Cardelli, J.A., Clayton, G.C. & Mathis, J.S. 1989, ApJ, 345, 245.
- Djorgovski, S.G., Kulkarni, S.R., Bloom, J.S., Goodrich, R., Frail, D.A., Piro, L., & Palazzi, E. 1998, ApJ, 508, L17.
- Djorgovski, S.G. et al. 2001, in Proceedings of the IX Marcel Grossmann Meeting, eds. V. Gurzadyan, R. Jantzen, and R. Ruffini, astro-ph/0106574.
- Djorgovski, S. G., Gal, R. R., Odewahn, S. C., DeCarvalho, R. R., Brunner, R., Longo, G. & Scaramella, R. 1999, in *Wide Field Surveys in Cosmology*, S. Colombi et al., eds., p. 89.

- Eisenhardt, P., Dickinson, M., Stanford, S.A., Ward, J., & Valdes, F. 1999, <http://iraf.noao.edu/iraf/ftp/contrib/dimsumV2/dimsum.readme>
- Fitzpatrick, E.L. & Massa, D. 1988, ApJ, 328, 734.
- Fox, D.W., Burruss, R., Berger, E., Bloom, J.S., Djorgovski, S.G., Kulkarni, S.R. & Haynes, M. 2001, GCN Circular 1099.
- Frail, D.A., Kulkarni, S.R., Nicastro, L., Feroci, M. & Taylor, G.B. 1997, Nature, 389, 261.
- Frail, D.A., et al. 2001, ApJ, 562, L55.
- Fukugita, M., Ichikawa, T., Gunn, J.E., Doi, M., Shimasaku, K. & Schneider, D.P. 1996, AJ, 111, 1748.
- Hurley, K. et al. 2001, GCN Circular 1097.
- Hogg, D., Cohen, J., Blandford, R., & Pahre, M. 1998, ApJ, 504, 622.
- Kennicutt, R.C. 1998, ARA&A, 36, 189.
- Kobulnicky, H.A., Kennicutt, R.C. & Pizagno, J.L. 1999, ApJ, 514, 544.
- Matthews, K., & Soifer, B.T. 1994, in *Infrared Astronomy with Arrays: the Next Generation*, ed. I. McLean (Dordrecht: Kluwer), 239.
- Mathis, J.S. 1983, ApJ, 267, 119.
- Oke, J.B. & Gunn, J.E. 1983, ApJ, 266, 713.
- Oke, J.B. & Gunn, J.E. 1982, PASP, 94, 586.
- Panaiteanu, A. & Kumar, P. 2001, ApJ (submitted), astro-ph/0108045.
- Park, H. S., Williams, G. G., Hartmann, D. H. et al. 2002, ApJ (submitted), astro-ph/0112397
- Persson, S.E., Murphy, D.C., Krzeminski, W., Roth, M. & Rieke, M.J. 1998, AJ, 116, 2475.
- Price, P.A. et al. 2001, ApJ, 549, L7.
- Price, P.A. et al. 2001, GCN Circular 1107.
- Reichart, D.E. 2001, ApJ, 553, 235.
- Ricker, G. R. et al. 2000, GCN Circular 839.



Ricker, G.R., et al. 2001a, GCN Circular 1096.

Ricker, G.R., et al. 2001b, in preparation

Sari, R., Piran, T. & Narayan, R. 1998, ApJ, 497, L17.

Schlegel, D.J., Finkbeiner, D.P., & Davis, M. 1998, ApJ, 500, 525.

Vreeswijk, P.M., et al. 2001, ApJ, 546, 672.

York, D. G., Adelman, J., Anderson, J. E. et al. 2000, AJ, 120, 1579.

Table 1. Optical observations of the afterglow of GRB 010921.

Date (UT)	Filter	Magnitude	Telescope	Lead Observer
2001 Sep 22.144	$r'$	$19.593 \pm 0.033$	P200 + LFC	Haynes/Burrus
2001 Sep 22.148	$r'$	$19.601 \pm 0.039$	P200 + LFC	Haynes/Burrus
2001 Sep 22.289	$I$	$18.854 \pm 0.064$	USNOFS1.0	Henden
2001 Sep 22.293	$R$	$19.669 \pm 0.060$	USNOFS1.0	Henden
2001 Sep 22.298	$V$	$20.296 \pm 0.070$	USNOFS1.0	Henden
2001 Sep 22.304	$B$	$21.159 \pm 0.088$	USNOFS1.0	Henden
2001 Sep 22.313	$U$	$20.910 \pm 0.205$	USNOFS1.0	Henden
2001 Sep 22.321	$R$	$19.790 \pm 0.069$	USNOFS1.0	Henden
2001 Sep 27.354	$r'$	$21.620 \pm 0.036$	P200 + LFC	Djorgovski
2001 Oct 12.226	$R$	$21.693 \pm 0.053$	P200 + LFC	Bloom
2001 Oct 17.145	$r'$	$21.994 \pm 0.028$	P200 + LFC	Mahabal
2001 Oct 17.165	$i'$	$21.660 \pm 0.022$	P200 + LFC	Mahabal
2001 Oct 18.088	$r'$	$21.918 \pm 0.030$	P200 + LFC	Mahabal
2001 Oct 18.110	$i'$	$21.670 \pm 0.021$	P200 + LFC	Mahabal
2001 Oct 19.178	$g'$	$22.947 \pm 0.043$	P200 + LFC	Mahabal
2001 Oct 19.109	$r'$	$21.977 \pm 0.028$	P200 + LFC	Mahabal
2001 Oct 19.130	$i'$	$21.650 \pm 0.030$	P200 + LFC	Mahabal
2001 Oct 19.149	$z'$	$21.419 \pm 0.043$	P200 + LFC	Mahabal
2001 Oct 19.253	$B$	$23.423 \pm 0.079$	P60	Fox
2001 Oct 19.206	$V$	$22.324 \pm 0.057$	P60	Fox
2001 Oct 19.272	$R$	$21.807 \pm 0.051$	P60	Fox
2001 Nov 01.287	$K_s$	$19.069 \pm 0.037$	KI + NIRC	Kulkarni
2001 Nov 01.345	$H$	$19.750 \pm 0.035$	KI + NIRC	Kulkarni
2001 Nov 01.316	$J$	$20.338 \pm 0.019$	KI + NIRC	Kulkarni

Note. — These measurements have not been corrected for Galactic extinction. The error in the measurement includes both statistical and systematic errors. A 2.5-arcsec aperture was used for optical measurements, and a 1.5-arcsec aperture for the NIR measurements. Telescopes are: P200 — Hale Palomar 200-inch; USNOFS1.0 — USNO Flagstaff Station 1.0-metre; P60 — Palomar 60-inch; KI — Keck I.

Table 2. Radio Observations of GRB 010921 made with the Very Large Array.

Epoch (UT)	$\nu_0$ (GHz)	$S \pm \sigma$ ( $\mu\text{Jy}$ )
2001 Oct 17.15	4.86	$188 \pm 25$
2001 Oct 17.15	8.46	$222 \pm 16$
2001 Oct 17.15	22.5	$330 \pm 90$
2001 Oct 18.23	8.46	$229 \pm 22$
2001 Oct 19.02	4.86	$100 \pm 28$
2001 Oct 24.02	22.5	$37 \pm 95$
2001 Oct 26.04	4.86	$91 \pm 36$
2001 Oct 28.99	4.86	$140 \pm 28$
2001 Oct 28.99	8.46	$158 \pm 26$
2001 Oct 29.99	8.46	$123 \pm 26$

Note. — The columns are (left to right), UT date of the start of each observation, observing frequency, and peak flux density at the best fit position of the radio transient, with the error given as the root mean square noise on the image.

Table 3. Lines identified in the spectrum of the host galaxy of GRB 010921.

$\lambda_{\text{obs}}$ (Å)	Line	$F_{\text{obs}}$	EW (Å)	GW (Å)	$F_{\text{corr}}$
5408.77±0.57	[O II]	2.42±0.23	50.1±5.1	11.5±1.1	24.4±2.3
5613.6	[Ne III]	< 0.98	< 13.8	...	< 8.9
7051.35±1.00	H $\beta$	0.69±0.11	13.2±2.3	10.2±1.9	3.12±0.50
7192.81±1.76	[O III]	0.41±0.13	9.2±3.0	10.8±3.3	1.75±0.55
7264.48±0.55	[O III]	2.18±0.14	43.5±3.5	12.9±1.1	9.11±0.59
9522.46±1.22	H $\alpha$	3.29±0.59	52±13	12.3±3.7	8.9±1.6

Note. — Left to right, the columns are the observed wavelength of the line, line identification, observed flux corrected for Galactic extinction using  $E_{(B-V)} = 0.148$ , observed equivalent width, observed Gaussian width and flux corrected for extinction in the host galaxy using an optical depth at H $\beta$  of 1.51 and an LMC extinction curve. Fluxes are in units of  $10^{-16}$  erg/cm<sup>2</sup>/s. Given the suggestion that GRB host galaxies may exhibit strong [Ne III] emission (Bloom, Djorgovski & Kulkarni 2001) we have included an entry for this line.

Table 4. Results of extinction curve fits to the optical afterglow photometry.

Afterglow Model	Collimated? yes/no	MW ( $c_2 = 2/3$ )		LMC ( $c_2 = 4/3$ )		SMC ( $c_2 = 7/3$ )	
		$A_V$ (mag)	$\chi^2$	$A_V$ (mag)	$\chi^2$	$A_V$ (mag)	$\chi^2$
$\nu < \nu_c, p = 3.1$	no	1.05	18.8	0.73	16.1	0.95	16.1
$\nu > \nu_c, p = 2.8$	no	0.76	16.8	0.52	15.5	0.66	15.5
$\nu > \nu_c, p = 1.6$	yes	1.29	21.0	0.89	16.7	1.17	16.8
$\nu < \nu_c, p = 1.6$	yes	1.75	26.0	1.20	17.7	1.60	18.0

Note. — The extinction curve formulation of Reichart (1999) was used in performing these fits. The models allow for both collimated ( $t_{jet} < 1$  d) and isotropic ( $t_{jet} > 25$  d) ejecta, and for the cooling break to be either redward ( $\nu > \nu_c$ ) or blueward ( $\nu < \nu_c$ ) of the optical bands over the period of observations of the afterglow ( $1 \text{ d} < t < 25 \text{ d}$ ).  $A_V$  is source frame V-band extinction; typical errors are 0.15 mag (MW), 0.10 mag (LMC) and 0.20 mag (SMC), not including co-variance. Each fit had 11 degrees of freedom.

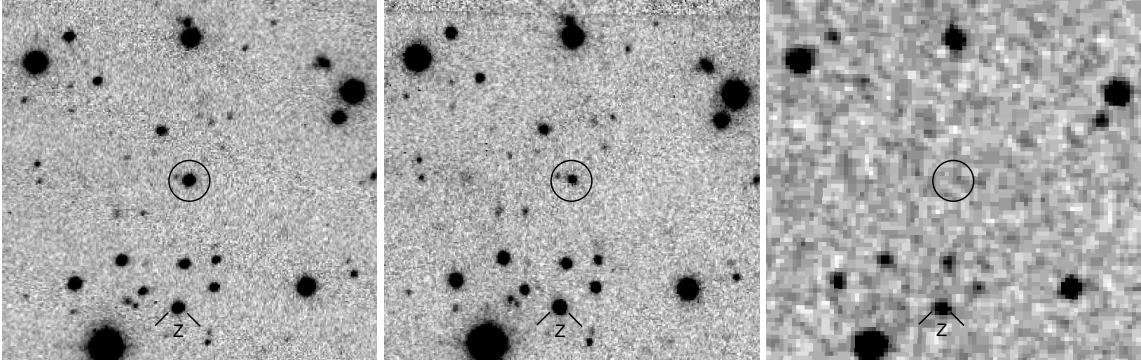


Fig. 1.— Identification of the optical afterglow of GRB 010921. Left and middle:  $r'$  images from the Hale 200-inch with the LFC on 2001 September 22 and 27 respectively. Right: Corresponding image from the DSS-2. Each image is 1.5-arcmin on a side, with North to the top and East to the left. The position of the optical afterglow is circled. Star Z (labeled), at coordinates  $22^{\text{h}}56^{\text{m}}00^{\text{s}}.2 + 40^{\circ}55'22''$  (J2000) is  $2.65''$  E and  $30.35''$  S of the afterglow, and for which we measure  $R = 21.169 \pm 0.043$  mag and  $I = 19.537 \pm 0.025$  mag.

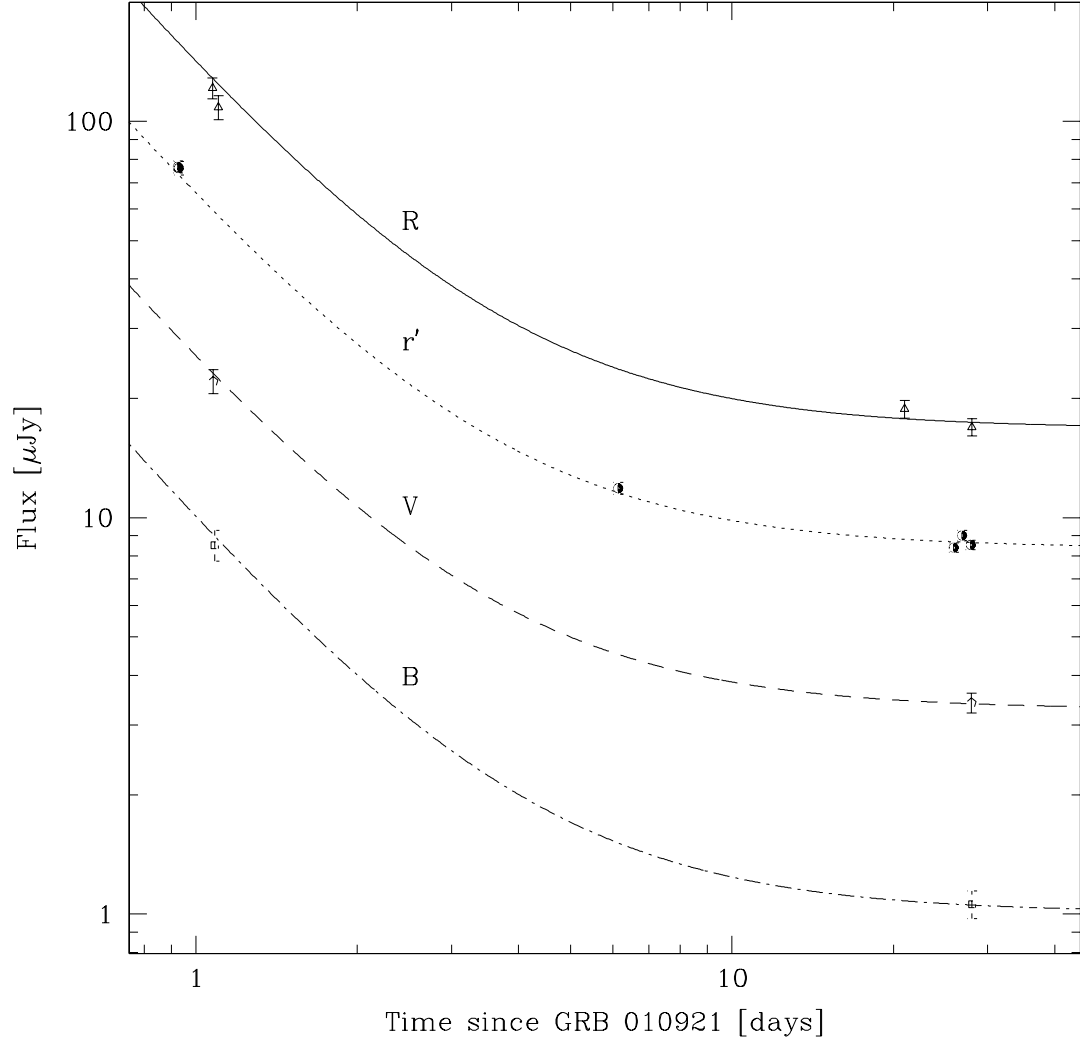


Fig. 2.— The optical light curve of the afterglow of GRB 010921. The displayed fluxes have been corrected for Galactic extinction using  $E_{(B-V)} = 0.148$ . The lines indicated the best-fit power-law plus galaxy model.

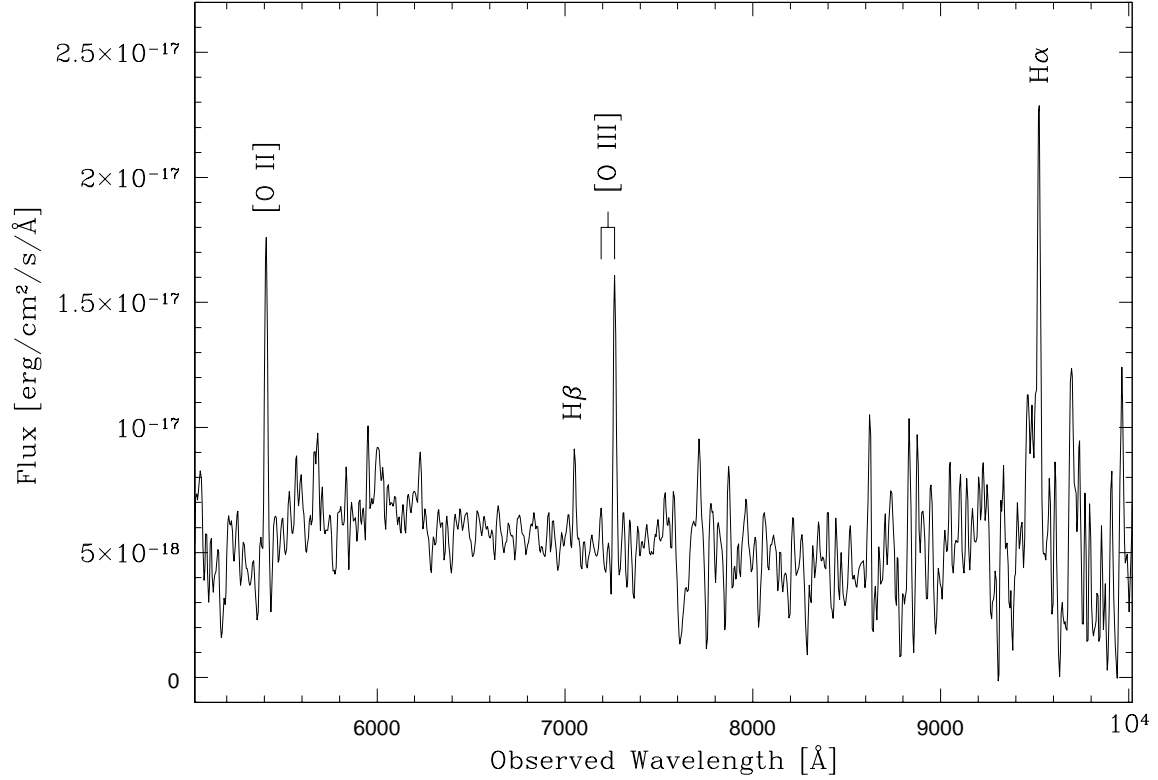


Fig. 3.— The spectrum of the host galaxy of GRB 010921. The spectrum has been smoothed with a Gaussian of FWHM = 12 Å, approximately the instrumental resolution. The continuum longward of 8500 Å suffers from poor sky subtraction. Emission lines corresponding to [O II], Hβ, [O III] and Hα (labeled) are clearly detected, corresponding to a mean redshift of  $z = 0.4509$ .